WIND TUNNEL INTERFERENCE EFFECTS ON A 70^o DELTA WING

M. R. Allan*, K. J. Badcock†, G. N. Barakos‡, and B. E. Richards§

Computational Fluid Dynamics Laboratory,

Department of Aerospace Engineering,

University of Glasgow,

G12 8QQ, United Kingdom.

URL: http://www.aero.gla.ac.uk/Research/CFD/ , Email : mallan@aero.gla.ac.uk

Keywords: CFD, Delta Wing, Tunnel Interference

Abstract

This paper considers the effects of both wind tunnel walls and a downstream support structure, on the aerodynamics of a 70^o delta wing. A RANS model of the flow was used with the wind tunnel walls and supports being modelled with inviscid wall boundary conditions. A consistent discretisation of the domain was employed such that grid dependence effects were consistent in all solutions, thus any differences occuring were due to varying boundary conditions (wall and support locations). Comparing solutions from wind tunnel simulations and simulations with farfield conditions, it has been shown that the presence of tunnel walls moves the breakdown location upstream. It has also been seen that vortex strength, helix angle, and mean incidence also increase, leading to a more upstream breakdown location in wind tunnels. The secondary separation line was also observed to move outboards. It was observed that for high Reynolds numbers, with a support downstream of the wing, vortex breakdown can be delayed due to blockage effects providing the vortices do not impinge on the support. This was observed to be the case for smaller supports also.

Nomenclature

S/W	Wing span (S) to tunnel width (W)
S/H	Wing span (S) to tunnel height (H)
c_r, c	Root chord
C_P	Pressure coefficient
M_∞	Freestream Mach number
U_∞, U_o	Freestream velocity
x	Chordwise distance
η	Spanwise distance / local span
ϕ	Helix angle
Γ	Circulation

*Research Assistant

†Senior Lecturer

‡Lecturer

§Mechan Professor

Introduction

WIND tunnels are used to test the aerodynamic characteristics of aircraft in the research and development stages. However, the influence of the tunnel walls must be taken into account when considering test results. Historically, wind tunnel corrections have been based on Linear Potential Flow Theory.[1] To obtain good quality and reliable test data, factors relating to wall interference, flow angularity, local variations in velocity, and support interference, must be taken into account. Karou[2] found that for delta wings with aspect ratio equal to one and spanning up to half the tunnel width, classical wall correction techniques can be used to correct flow field and force results up to 30^o angle of attack (it should be noted that vortex breakdown was unlikely to be present over the wing). Also, for swept wings with a blockage ratio (ratio of model planform area to tunnel cross-sectional area) of less than 0.08, tunnel interference effects can usually be considered negligible.[3]

Clearly, the flow conditions within a wind tunnel will be different to those a wing would experience in free air. The interactions between the wing and wall flow fields induce longitudinal and lateral variations (streamline curvature and aerodynamic twist respectively) to the freestream, in addition to those attributed to the wing alone. These differences may result in a reduction in the average downwash experienced by the model, a change in the streamline curvature about the model, an alteration to the local angle of attack along the span of the model, a change in dynamic

pressure about the model due to solid and wake blockage, and in the buoyancy effect due to the axial pressure gradient along the tunnel test section. The magnitude of these effects increases with model size (increasing solid blockage).

Weinberg[4] conducted an experimental investigation into wall effects. He tested two sets of three wings (one set with 60^o sweep, and one set with 70^o sweep), each wing with a different span size. The experiment was performed in a square water tunnel (low Re) at a constant flow velocity of 11m/s. The tunnel size was 45cm x 45cm. He found that for the three wings with 70^o sweep, as the wing size was increased (kept at a constant angle of attack), vortex breakdown moved downstream. For the three wings with 60^o sweep, he found that as the wing span-to-tunnel width ratio increased from 0.175 to 0.35, the wall effects followed the computed trends (i.e. vortex breakdown was shifted downstream with increasing wing size). However, when the wing span-to-tunnel width ratio was increased from 0.35 to 0.7, no significant change was observed. This suggested that effective camber was not the only influence. For both the 60^o and the 70^o wings, the difference in breakdown location observed from the smallest model to the largest model, was of the order $25\%c_r$.

Thompson and Nelson[5] investigated experimentally the influence of tunnel walls on a 70^o delta wing by testing full, two thirds, and half scale models in a square tunnel (the largest model gave the ratios S/H = S/W = 0.364). Due to a steady hysteresis effect the wing was tested for a quasi-steady upward and downward stroke. It was found that for the smallest model tested (S/H = S/W = 0.124) the breakdown location shifted downstream by as much as $15\%c_r$ on both the quasi-steady upstroke and downstroke. For the half scale model and the full scale model, there appeared to be little difference in the breakdown locations. As stated by Thompson and Nelson, this shift downstream as model size is decreased is in contrast to the results of Weinberg.[4] It was noted that Weinberg used a Reynolds number an order of magnitude lower, and a constant velocity, as opposed to keeping the Reynolds number constant (as in the experiments of Thompson and Nelson). It was observed that the vortex suction on the model surface increased with model size.

More recently Pelletier and Nelson[6] studied the effect of tunnel interference on 70^o delta wings. Experiments were conducted in a water tunnel with three different sized wings. These low Reynolds number tests agreed with the previous findings of Thompson and Nelson[5] who tested at higher Reynolds number, in that breakdown moved towards the apex with increasing wing size. Pelletier and Nelson used the method of images to explain this effect, concluding that the tunnel walls increased the mean incidence of the wing, thus promoting breakdown.

Verhaagen et al.[7] performed Euler calculations of the flow over a 76^o delta wing inside wind tunnels of increasing size. The wing span-to-tunnel width ratios considered were 0.292, 0.389, and 0.584 and the test section was octagonal. To model the effect of a secondary separation, a small "fence" was placed where secondary separation would occur. It was found that decreasing the tunnel size (increasing the wing span-to-tunnel width ratio) increased the suction in the vortices and increased the velocities in the vortex core, due to an increase in circulation with decreasing tunnel size.

Allan et al.[8] performed Euler simulations of tunnel interference effects on a 65^o delta wing in various tunnels for static and pitching cases. It was observed that tunnel side walls were the most influential factor on breakdown location, with roof and floor having little effect. It was also noted that in pitching simulations, the tunnel interference effects were strongest on the downstroke, during the vortex reformation.

When considering support interference effects Hummel[9] observed that the presence of an obstacle one chord length downstream of the trailing edge of a delta wing caused vortex breakdown to shift towards the apex by up to $40\%c_r$. The obstacle considered was unrealistically large (wider than the span of the delta wing), however, this early observation highlighted the possible effects that support structures can have. Recently Taylor et al.[10] varied the position of various obstacles behind the wing's trailing edge to find the effect support proximity had on vortex breakdown. It was concluded that when an obstacle was placed in the vortex core, breakdown was promoted due to the adverse pressure gradient which formed in front of the obstacle. As the obstacle was moved away from the vortex core, breakdown was observed to move downstream. It can be expected that the degree of support interference will be dependent on support size, vortex strength and trajectory. Although possibly not considered as support interference, fuselages on delta wing models can effect the breakdown location. Some sting mounted tunnel models have upper surface fuselages to connect the model to the sting. The effect of such fuselages has been considered in a number of investigations, each of

which have shown significant variations in breakdown location for a given sweep angle and incidence. See for example[11 12].[13] A possible reason for the variation in the breakdown locations was given by Ericsson[12] in which the effect of the fuselage was described as an induced camber effect. The induced camber effect alters the location of vortex breakdown, either delaying or promoting breakdown depending on the fuselage.

In view of the above, three dimensional Navier-Stokes computations are necessary to correctly predict the complex leeward side flow characteristics of delta wings. RANS simulations of tunnel interference on a 70^o delta wing have been conducted and the results are presented in the current paper. Support structure interference has also been considered.

Computational method

All simulations described in this paper were performed using the University of Glasgow PMB3D (Parallel Multi-Block 3D) RANS solver. A full discussion of the code and turbulence models implemented is given in.[14] PMB3D uses a cell centered finite volume technique to solve the Euler and Reynolds Averaged Navier-Stokes (RANS) equations. The diffusive terms are discretised using a central differencing scheme and the convective terms use Roe's scheme with MUSCL interpolation offering third order accuracy. Steady flow calculations proceed in two parts, initially running an explicit scheme to smooth out the flow solution, then switching to an implicit scheme to obtain faster convergence. The pre-conditioning is based on Block Incomplete Lower-Upper (BILU) factorisation and is also decoupled between blocks to help reduce the computational time. The linear system arising at each implicit step is solved using a Generalised Conjugate Gradient (GCG) method. For time-accurate simulations, Jameson's pseudo-time (dual-time stepping) formulation is applied, with the steady state solver used to calculate the flow steady states on each physical time step (discussed fully in[14]).

Since the RANS equations are solved the 2 equation k-ω model is used for closure. It is well known that most linear 2-equation turbulence models over-predict the eddy viscosity within vortex cores, thus causing too much diffusion of vorticity.[15] This weakens the strength of the vortices and can eliminate secondary vortices, especially at low angles of attack where the vortices are already weak. The following modification suggested by Brandsma et al.[16] was therefore applied to the standard k-ω model of Wilcox[17] to reduce the eddy-viscosity in vortex cores.

$$P_k = min\{P_k^u, (2.0 + 2.0min\{0, r-1\})\rho\beta^* k\omega\} \quad (1)$$

Here P_k^u is the unlimited production of k, P_ω^u is the unlimited production of ω, and r is the ratio of the magnitude of the rate-of-strain and vorticity tensors. When k is over predicted in the vortex core, it will be limited to a value relative to the dissipation in that region. This modification was found improve predictions compared with the standard k-ω turbulence model.[18]

The Computational Fluid Dynamics Laboratory at the University of Glasgow owns a cluster of PC's. The cluster is known collectively as Jupiter and is fully described by Badcock et al.[14] There are 32 nodes of 750MHz AMD Athlon Thunderbird uni-processor machines, each with 768Mb of 100MHz DRAM. MPI (Message Passing Interface) is used to link up multiple nodes to create a virtual machine, which is used to execute computationally demanding problems. PMB3D balances the node loadings (number of cells per node) by spreading the blocks over all the nodes of the virtual machine. Halo cell values are passed between adjacent blocks using MPI.

Test case : ONERA 70^o Wing

The subsonic case of a 70^o delta wing is considered at 27^o angle of attack. At this incidence vortex breakdown is occurring over the wing. The wing has a root chord length of 950mm, a trailing edge length of 691.5mm, flat upper and lower surfaces, and a leading edge bevel of 15^o. The wind tunnel model had a blunt trailing edge 20mm thick which has been beveled (15^o bevel) in the computational model to simplify grid generation. Experimental data was obtained by Mitchell.[19] The wing was tested in the ONERA F2 tunnel (situated at Le Fauga-Mauzac Center, near Toulouse, France) which has a working section of height 1.8m, width 1.4m, and length 5m. It is a subsonic, continuous, closed-return tunnel. The wing was also tested in the ONERA S2Ch tunnel situated at the Chalais-Meudon Centre (ONERA) which is of quasi-circular cross-section with a diameter of 3m and a test section length of 4.93m. The model/tunnel ratios are S/W=0.49 and S/H=0.38 for the ONERA F2 tunnel, and S/W=0.23 and S/H=0.55 (taking into account off tunnel centreline location of wing) for the ONERA S2Ch tunnel. Despite the flow conditions being similar in both tunnels, the mean break-

Tunnel	S/W	S/H	M_∞	Re
Farfield	-	-	0.2	1.56×10^6
ONERA F2	0.49	0.38	0.2	1.56×10^6
S/W = 0.63	0.63	0.38	0.2	1.56×10^6

Table 1 ONERA 70^o wing test cases - Fully turbulent flow.

down locations were closer to the apex in the ONERA F2 tunnel (the smaller of the two), when compared with those measured in the ONERA S2Ch tunnel. This suggests some test facility interference, which could be due to either the support structure or tunnel wall interference.

The flow conditions for which extensive experimental data from the ONERA F2 tunnel are available are an incidence of 27^o, Reynolds number of 1.56×10^6, and a freestream velocity of 24m/s ($M_\infty = 0.069$). For these flow conditions, flow visualisation of velocity components, vorticity components, turbulent kinetic energy components and local static pressure are available in various planes. Vortex breakdown locations were also obtained based on where the axial component of velocity becomes negative. In the simulations the Reynolds number has been matched, however the Mach number is 0.2, compared with the lower Mach number of 0.069 in the experiment. Since the current work is based on a high speed flow solver, a freestream Mach number of 0.2 was used to avoid any possible convergence issues. Transition was observed to occur at around $40\%c_r$ in experiment, however the CFD simulations assume a fully turbulent flow.

Three boundaries have been chosen. The first has the wing in free air (farfield), the second represents the ONERA F2 tunnel, and the third the ONERA F2 tunnel side walls brought closer to the wing (increasing the S/W ratio). Full details of these configurations as well as flow parameters can be found in Table 1.

To try and assess the effects of support structures a vertical generic support was placed in the centre of the ONERA F2 tunnel downstream of the wing. Since supports in dynamic testing tend to be fairly large (driving mechanisms must also be housed) a thick support cross-sectional area was chosen. The generic support considered is a cylinder with a straight taper in the downstream direction. Figure 1 shows the support structure and dimensions. To avoid grid generation complications, the support attaching the wing to the vertical support is omitted. It may be expected that there is some interference from this mounting. The downstream support gives a frontal area blockage of around 12%.

The support was placed at two locations in the

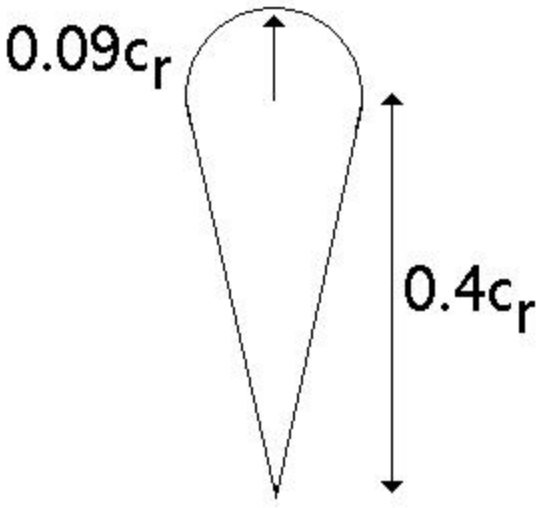

Fig. 1 ***Support geometry and dimensions.***

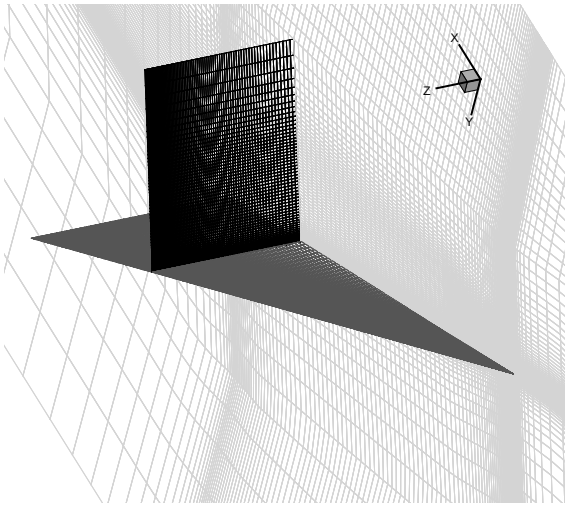

Fig. 2 ***ONERA 70^o wing, View of ONERA F2 tunnel mesh.***

ONERA F2 tunnel case, at $0.5c_r$ and $1c_r$ from the trailing edge of the wing. The grids over the wing used for the support interference simulations are identical to those for the ONERA F2 tunnel without supports. Therefore there is no change in grid resolution in the vortical region above the wing. The ONERA F2 tunnel mesh was altered downstream of the wing to allow the presence of the support. In all cases the tunnel walls have been modelled with an inviscid wall boundary condition, and in the support structure simulations the supports have also been modelled with an inviscid wall boundary condition. Neglecting wall and support structure boundary layers reduces the mesh sizes significantly.

Computational grids

The ONERA 70^o wing inside the ONERA F2 tunnel is considered. A depiction of the grid around the ONERA 70^o wing is given in figure 2. The mesh is of H-H topology with only half the wing modelled, and the wing has been meshed at 27^o. The tunnel grids have been extracted from the "farfield" grid by removing outer blocks so that the mesh resolution over the wing is identical in each case. The first cell height normal to the wing surface is $10^{-6}c_r$. This yields an average y^+ value of less that 1.0. The mesh sizes are given in Table 2. All grids had 99 points streamwise and 79 points spanwise over the wing.

Test case	Normal to upper surface	Total
Farfield	117	3,969,810
ONERA F2	103	2,904,660
S/W=0.63	103	2,664,090

Table 2 Viscous grid dimensions.

Verification and validation

The solutions described in this paper have been validated in.[18] Therefore only a brief discussion is presented here. In order to validate and assess the predictions of the modified k-ω model, the ONERA 70^o wing inside the ONERA F2 tunnel is considered. In order to attempt to verify the accuracy of the solutions, a limited grid dependency study has been conducted. Due to the high computational power requirements to solve the flow with the fine grid, only a comparison with the coarse grid solution is presented. The "coarse" grid is created by extracting a level in each direction from the standard grid. The upper surface pressure distributions are given in figure 3. The breakdown locations from the coarse and standard grids are $59.6\%c_r$ and $64.7\%c_r$ respectively. Clearly as we go from the coarse to standard grids the suction peaks increase in strength and vortex breakdown moves downstream.

Flow visualisation of the solutions indicates that a grid refinement increases the core properties (higher suction, higher axial velocities, higher vorticity) and increases turbulence levels within the vortex. Clearly as breakdown is delayed going from the coarse to the standard grid, the increase in the core properties is dominant over the dissipation of kinetic energy in the vortex, allowing the core flow to negotiate the adverse pressure gradient a little further. It should be noted that Visbal and Gordnier[20] observed for simulations on a 75^o delta wing at 25^o

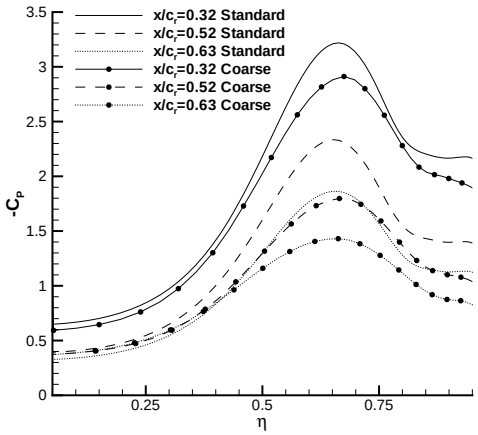

Fig. 3 ***Dependency of upper surface pressure distribution with grid refinement.***

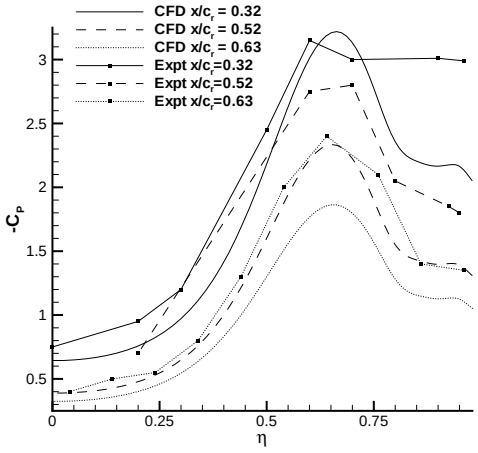

Fig. 4 ***Comparison of upper surface pressure distribution with experiment.***

angle of attack, with Reynolds number equal to 2×10^6, and freestream Mach number of 0.2, that on a coarse grid (H-H topology) vortex breakdown was located upstream to that computed on a finer grid. Since the grids used for the tunnel calculations have been extracted from a common farfield grid, the grid dependency of each solution will be similar. As such, despite the fact that further refinement of the vortices is required (which is not currently feasible due to computing limitations), the grid dependency is equal for all cases, and therefore solution to solution comparisons for tunnel effects is still valid.

In all solutions the mean flow residual converged at least four orders of magnitude. If we look at the upper surface pressure distributions at the chordwise stations of $x/c_r = 0.32$, 0.52, and 0.63 (figure 4), we see reasonable agreement

of the experimental and predicted flow structures, with the presence of a primary and secondary vortex. It is also clear that the variation in the strength of the footprint in the chordwise direction reduces faster in the CFD solutions in comparison to experiment. This may be due to the vertical position of the vortex being poorly predicted (possibly due to the laminar / turbulent transition in experiment varying the position of the vortex core), or that the grid resolution is insufficient. It should be noticed that the H-H mesh topology expands the cell sizes in the chordwise direction along a delta wing. However, in general the upper surface pressure distributions are predicted well especially close to the apex. The suction levels near the apex (where the flow is highly resolved) compare well with experiment, despite the strength of the secondary vortex possibly being under-predicted. It should be recalled, however, that in the experiment the flow is laminar until around $40\%c_r$, which may explain the weaker secondary vortex near the apex (due to turbulence effects). Further downstream, the structure of the vortex is visible despite the vortex footprint weakening faster in comparison to experiment.

Although not presented, the distribution of the core axial velocities was also compared with experiment. It was observed that the peak core velocities were around 2.5 times freestream, compared with 3.5 times freestream in experiment. Such a deficit is common in CFD simulations. The core vorticity levels were also compared with experiment, as were the helix angles, and good agreement was found.

Results - No support

In order to obtain the breakdown locations above the ONERA 70^o wing, the location at which the axial component of velocity becomes zero was used. This is consistent with the method used in experiment. To achieve this, a vertical slice through the vortex core was taken and the point where the axial velocity becomes zero was measured. The breakdown locations for the three test cases are given in Table 3.

The promotion of vortex breakdown is comparable in magnitude (though a little lower) to the promotion of vortex breakdown seen experimentally when going from the larger ONERA S2Ch tunnel to the smaller ONERA F2 tunnel. It should be kept in mind that support effects have been omitted in the CFD solutions. As in the Euler simulations of Allan et al.,[8] increasing the S/W ratio has the effect of promoting vortex breakdown.

TUNNEL	S/W	S/H	Breakdown Location
Farfield	-	-	$68.8\%c_r$
ONERA F2	0.49	0.38	$64.7\%c_r$
S/W=0.63	0.63	0.38	$60.3\%c_r$
Experiment			
ONERA F2	0.49	0.38	$65\pm5\%c_r$
Experiment			
ONERA S2Ch	0.23	0.55	$\approx72\%c_r$

Table 3 Summary of steady breakdown locations for ONERA 70^o wing at 27^o angle of attack.

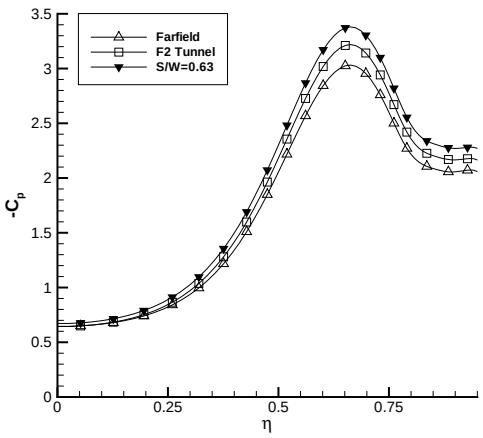

Fig. 5 ***Comparison of upper surface pressure distributions,*** $x/c_r = 0.32$.

Figures 5 to 7 show the spanwise surface pressure distributions at the chordwise locations of $x/c_r = 0.32$, $x/c_r = 0.52$, and $x/c_r = 0.63$ respectively. Examination of the secondary separation location (taken to be where the spanwise shear stress component changes sign) indicates that the presence of wind tunnel walls causes the secondary separation line to move outboard, with the displacement increasing in extent in the chordwise direction. The reason for this is discussed later. When the flow is confined by the ONERA F2 tunnel, the primary suction peak increases, and increases further as the side wall is brought closer (the S/W=0.63 tunnel). It can also be seen that the secondary vortex increases in strength (almost equally in comparison to the primary suction peak) with increasing S/W.

The tunnel wall pressure distributions on the ONERA F2 and the S/W = 0.63 tunnels are shown in figure 8. It is clear that there is a strong vortical flow pattern on the side walls which extends down the tunnel despite vortex

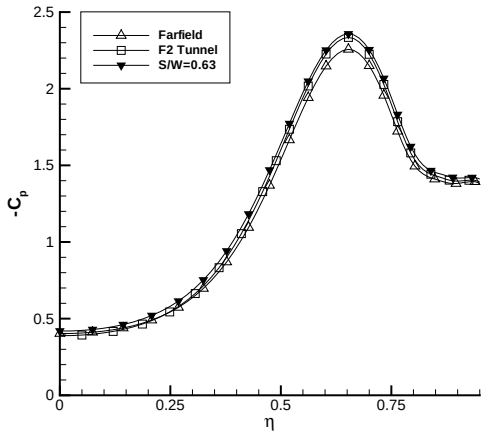

Fig. 6 *Comparison of upper surface pressure distributions,* $x/c_r = 0.52$.

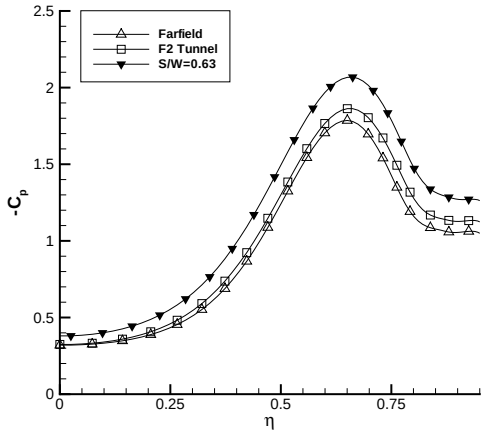

Fig. 7 *Comparison of upper surface pressure distributions,* $x/c_r = 0.63$.

breakdown having occured (the persistence of vortical flow despite breakdown occuring was also observed during experiments). The flow patterns appear similar for the ONERA F2 tunnel and the S/W=0.63 tunnel, however the strength of the pressure distribution increases with increasing S/W ratio. Clearly there is a significant amount of interference induced by the side walls.

In order to assess the adverse pressure gradient experienced by the vortex core, the pressure distribution along the vortex core in each tunnel is shown in figure 9. Visbal[21] found that vortex breakdown was heavily dependent on the pressure gradient along the vortex core. As the wing is placed in a wind tunnel, the suction in the vortex core prior to breakdown increases. This implies that when the vortices are placed within wind tunnels, they become stronger than those in

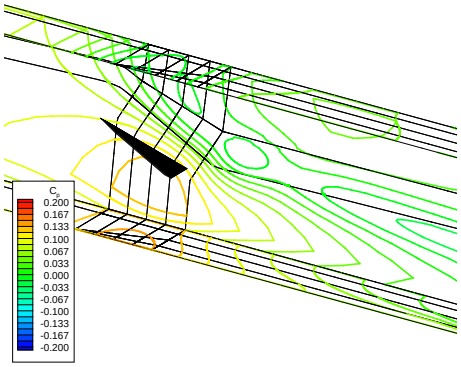

(a) ONERA F2 tunnel

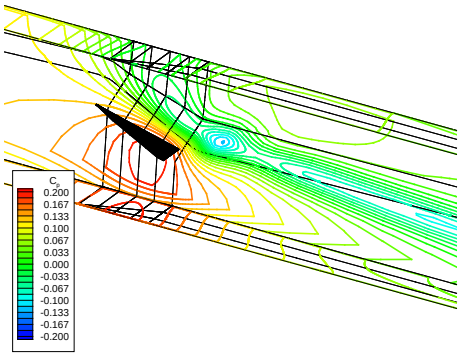

(b) S/W = 0.63 Tunnel

Fig. 8 *Steady flow tunnel wall pressure distributions.*

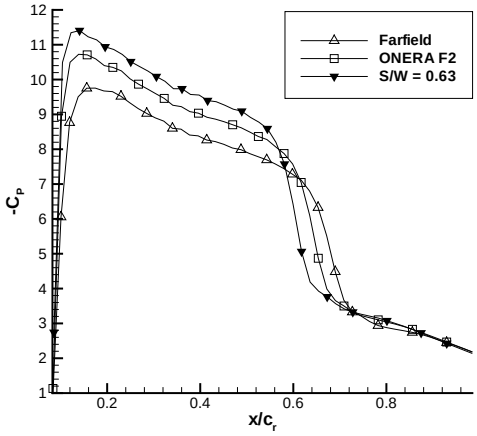

Fig. 9 *ONERA* 70^o *wing, Pressure distributions along vortex cores.*

farfield conditions. With this additional suction the adverse pressure gradient experienced by the core flow increases, thus vortex breakdown is expected to be promoted. This agrees qualitatively with the results of Visbal.

The flow angle (the angle at which the

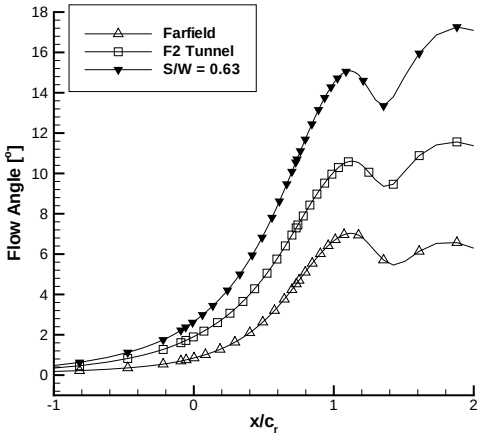

Fig. 10 *ONERA* 70^o *wing, Flow angles at 1.5 wing span lengths from wing.*

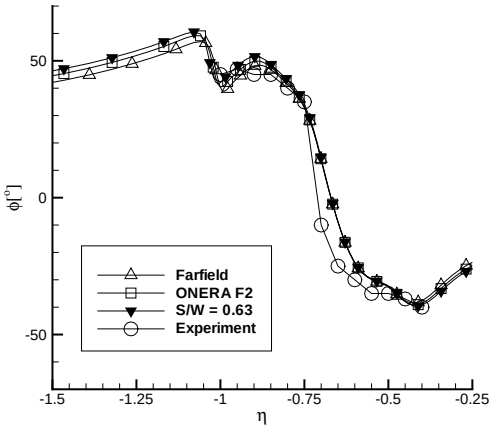

Fig. 11 *ONERA* 70^o *wing, Comparison of helix angles through vortex cores at* x/c_r*=0.52.*

freestream is turned up due to the presence of the wing and side walls) variation in the streamwise direction can be seen in figure 10. Both tunnels increase the flow angle ahead of the wing in comparison to the farfield solution, and also increase the rate at which the flow angle increases along the wing. There are two possible effects present, an increase in the mean effective incidence and induced camber. Both these effects increase with increasing S/W. Since breakdown has moved towards the apex it is expected that the increase in the mean effective incidence is the dominant effect.

Figures 11 shows the distribution of the helix angle through the midline of the vortex core at the chordwise location of $x/c_r = 0.52$. At this chordwise location the vortex is unburst in all solutions. The experimental helix angle obtained in the ONERA F2 tunnel[19] is also given for comparison. As the tunnel walls are brought closer to the wing it can be seen that the helix angle increases (the turns of the vortex tighten) which can cause a promotion of vortex breakdown.[22] This is due to the side wall induced vertical velocity components which also increase in the mean effective incidence of the wing. The tightening of the vortex increases the crossflow momentum. Given that the adverse pressure gradient experienced by the wing boundary layer as it passes from beneath the primary vortex core to the secondary separation region, is unchanged (the secondary suction also increases with the primary suction), the likely cause of the delay in secondary separation in the tunnels is an increase in crossflow momentum due to the tighter winding of the vortex. It can also be seen that the location at which the helix angle changes sign (as we pass through the vortex core) does not appear to move significantly with increasing S/W ratio, indicating the vortex core does not move spanwise significantly at this chordwise station.

The static pressure distribution along the centreline of the tunnels and the farfield solution can be seen in figure 12. As the centreline passes through the wing the switch from the pressure side to the suction side can be seen as a jump in the curve at approximately x/c_r=0.75. It is evident that as the tunnel size decreases the static pressure beneath the wing increases (as expected due to increasing frontal area blockage). The suction over the wing upper surface also increases with decreasing tunnel size. The effect of the lifting of the broken down vortex system into the centre of the tunnel can also be seen. Behind the wing the tunnel pressure distributions are slightly above that of the farfield. However, it should be recalled that there are two effects, the blockage increasing the static pressure within the tunnel, and the vortex lifting which decreases the pressure in this region. Thus it is the difference between the pressure increment ahead of the wing and behind the wing that shows the extent of the vortex lifting. The displacement of the vortices has been confirmed with flow visualisations.

The chordwise variation in circulation along the vortex is given in figure 13. The circulation was obtained by integrating the ω_x component of the vorticity vector over ten chordwise slices. The oppositely signed secondary separation region was omitted (which would have the effect of lowering the circulation). From the apex to around the midchord position it can be seen there is a relatively linear growth in circulation

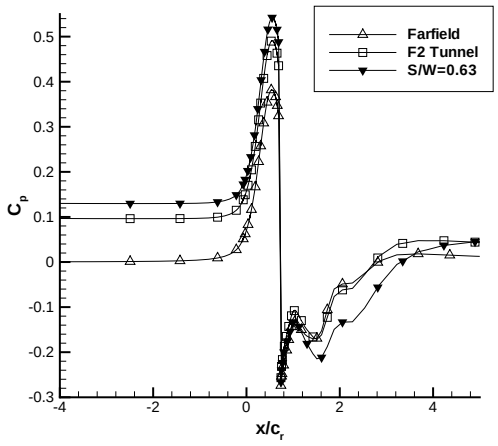

Fig. 12 ***ONERA*** 70^o ***wing, Tunnel centreline pressure distributions.***

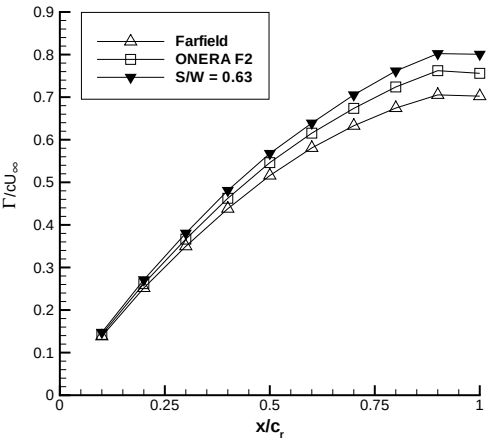

Fig. 13 ***ONERA*** 70^o ***wing, Comparison of circulation distributions.***

in the chordwise direction, after which the rate of growth in circulation decreases.[23] Despite vortex breakdown occurring the circulation continues to increase in the chordwise direction,[24] eventually becoming near constant as the trailing edge is reached. The integrations were performed over an entire extracted plane, thus it would appear rather than there being a loss in the ω_x component of vorticity, it is dispersed throughout the vortex. If the integration region is not large enough to encompass this dispersion, it may appear that there is a loss in circulation. The circulation curves further indicate that as the wing is placed in wind tunnels the vortices become stronger, strengthening with increasing S/W ratio.

Results - With supports

Incidence	Support location	Breakdown location
27	$0.5c_r$	$81.0\%c_r$
27	$1c_r$	$65.9\%c_r$
27	NONE	$64.7\%c_r$

Table 4 Vortex breakdown locations with and without supports.

The breakdown locations observed in the calculations are given in table 4. The breakdown locations have been taken where the axial velocity equals zero.

It can be seen that when the support is $1c_r$ from the trailing edge there appears to be a small influence on breakdown, with breakdown being delayed slightly in comparison to the case without support structures. Since the vertical support used in the experiments of Mitchell[19] was placed around $2c_r$ from the trailing edge of the wing, it can be safely concluded that its interference effect on the experimental breakdown location is minimal. As the support is brought closer to the trailing edge of the wing (at $0.5c_r$ from the trailing edge) it can be seen that breakdown shifts back towards the trailing edge by around $16.3\%c_r$. This is in contrast to what may be considered as the common understanding that downstream supports induce vortex breakdown due to pressure disturbances propogating upstream.

To find the reason for the tendency of this support to delay vortex breakdown, the structure of the vortices prior to breakdown was examined (for a full discussion see[18]). The flow angles (the angle at which the freestream is deflected due to the presence of the wing) were examined and it was observed that there is little change when supports are placed in the tunnel. This is due to the flow angles only being altered by the proximity of the vortices to the side wall (which induce vertical velocity components increasing the mean incidence of the wing). Indeed provided the vortices do not increase in strength due to the supports, the flow angles should remain the same. The surface pressure distributions above the wing at x/c_r =0.32, 0.52, and 0.63 were also examined and again there was little difference, both in core location and strength. The axial vorticity distributions and chordwise distribution of circulation was finally examined and it was concluded that prior to breakdown, the support structures had no influence on the vortex structure.

Figures 14 and 15 shows the pressure distribution along a horizontal plane at the midpoint between the tunnel roof and floor for each inci-

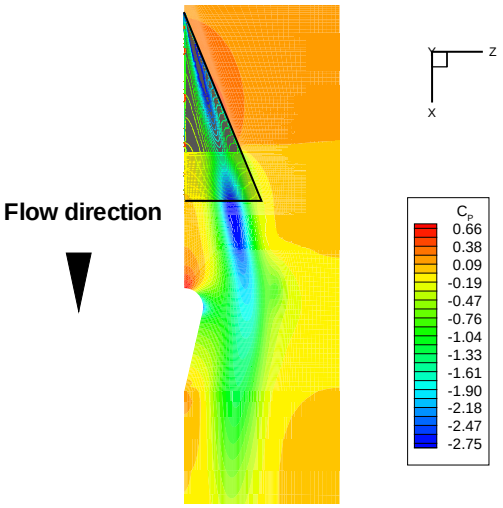

Fig. 14 *Pressure distribution along a horizontal plane, support $0.5c_r$ from wing trailing edge.*

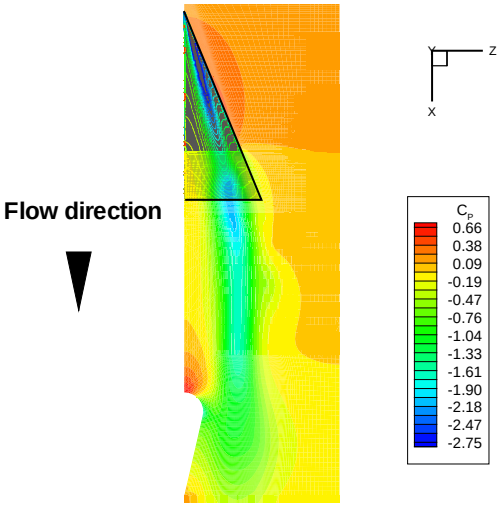

Fig. 15 *Pressure distribution along a horizontal plane, support $1c_r$ from wing trailing edge.*

dence and support location. The flow direction is from top to bottom and the intersection of the horizontal plane with the wing is clearly seen upstream of the support. Evidentally the vortical flow negotiates the support as opposed to impinging on it as in the experiments of Taylor et al.[10 25] Since the mean effective incidence of the wing and strength of the vortices is unaltered prior to vortex breakdown, the only explanation for the delay in vortex breakdown is the change in the pressure gradients in the tunnels. It is well understood that vortex breakdown is sensitive to external pressure gradients.[26]

Examination of the tunnel axial pressure gradients indicates that as the support is brought near the wing, a local (to the wing) favourable pressure gradient develops. It should be noted that the pressure gradient at the side wall was examined, not the pressure gradient along the centreline of the tunnel which would incorporate an adverse pressure gradient as the support is approached. Since the vortices do not impinge on the support, they will not experience this adverse pressure gradient, therefore the pressure gradient at the side wall is more indicative of the pressure gradient experienced by the vortices. The favourable pressure gradient is due to an acceleration of the flow as it negotiates the support, thus reducing the local static pressure around the support. To have an effect on vortex breakdown the favourable pressure gradient must be local with respect to the vortices, and so when the support is placed $1c_r$ from the wing, the favourable pressure gradient around the support has a smaller effect.

From the previous discussion it is clear that downstream support structures have the sole effect of altering the pressure gradients within the tunnel. There is little or no change to the vortex structure prior to vortex breakdown. Clearly the shape and size of the support considered in this study alters the pressure gradients in the tunnels due to blockage effects. The acceleration of the flow around the support causes a favourable pressure gradient to form, and if this pressure gradient is local with respect to the vortices breakdown is delayed. However there is also a stagnation region ahead of the support so it is possible that if the blockage effect was lower, the stagnation effect may become dominant and breakdown will be promoted. To assess any possibility of this a narrower support was placed at $0.5c_r$ from the trailing edge of the wing, with the wing at 27^o angle of attack. The geometry is identical to that described in figure 1, however the radius of the cylindrical section was reduced from $0.09c_r$ to $0.045c_r$. This effectively halves the support frontal area blockage from approximately 12% to 6%. The breakdown was observed to shift from $64.7\%c_r$ to $73.8\%c_r$. Clearly despite the blockage being reduced the previous discussion applies to thinner supports. As long as the vortex cores negotiate the support breakdown can be delayed. This seems to be the case for "streamlined" tunnel-centred support structures at high Reynolds number. The effect of the favourable pressure gradient at low Reynolds number is likely to be lower.

Conclusions and future work

A CFD investigation of wind tunnel interference effects on a 70^o delta wing has been con-

ducted. The vortical flow predictions were verified and validated, and then used to analyse the effects of wind tunnel walls. Verification of the accuracy on the grids employed has highlighted a dependency of the solutions to grid resolution. From the available literature this has been found to be common in the prediction of vortical flows. To ensure that any differences are only due to changes in boundary conditions (such as locations of tunnel walls and support structures), in all computations the vortical region of interest has been resolved with a consistent discretisation of the domain. To achieve this a farfield grid was created in such a way that by extracting outer blocks varying tunnel dimensions were obtained.

RANS simulations have confirmed previous conclusions drawn from Euler simulations.[8] It has been observed that the amount of upwash generated (and therefore the mean effective incidence) is dependent on the side wall location. As the side wall moves closer to the wing, the local effective incidence along the leading edge increases. Since the local effective incidence of the wing increases along the leading edge (tunnel interference increases toward the trailing edge as the vortices are closer to the side walls), the wing might be considered to behave as if positively cambered. A positively cambered wing is expected to delay vortex breakdown. Since breakdown is promoted it appears that the increase in mean effective incidence is the dominant factor. The helix angle of the vortices also increases due to side wall proximity. The side wall induced upwash tightens the windings of the vortex and therefore increases the vortex strength. Higher helix angles are known to induce vortex breakdown.

The influence of the tunnel side walls on the secondary vortices was also assessed. It was observed that the secondary separation location moves towards the leading edge when the wing is placed inside wind tunnels. The helix angle of the vortices increases with the presence of the tunnel side walls. This increases the strength of the primary vortices due to the increased crossflow momentum (a result of the tighter windings). However, the increased crossflow momentum also increases the strength of the secondary region, thus the adverse pressure gradient experienced by the crossflow after the primary vortex suction peak is essentially unaltered. With the increased crossflow momentum the adverse pressure gradient can be overcome longer, and therefore the secondary separation line moves outboard.

In order to assess support interference a support with a large frontal area blockage was used. The support was placed at two chordwise locations in order to assess the effect of support proximity on the solutions. It was observed that the leading edge vortices were very sensitive to variations in pressure distributions aft of the trailing edge, due to the presence of supports. In addition the downstream support structures had no effect on the flow structure prior to vortex breakdown. The support shape considered caused a significant acceleration of the flow due to blockage which had the effect of delaying vortex breakdown. This trend was observed irrespective of support width (frontal area blockage). The trajectory of the vortex cores was such that the core flow never experienced the adverse pressure gradient ahead of the support structure. Thus it can be concluded that the effect of downstream support structures is heavily dependent on whether or not the core flow impinges on the structure, and is also likely to be dependent on Reynolds number.

Since turbulence modelling plays a significant role in the prediction of vortical flows, the work presented should be considered a qualitative assessment of tunnel interference effects. In order to improve the accuracy and validate further the predictions, time-accurate simulations and more advanced turbulence modelling (such as Detached Eddy Simulation) should be employed.

ACKNOWLEDGEMENTS

The authors wish to thank Major A. Mitchell, United States Airforce Academy, for kindly providing the experimental data. The financial support from QinetiQ Ltd (formerly DERA Bedford) is gratefully acknowledged.

References

[1]Garner, H. C., and Rogers, E. W. E. "Subsonic wind tunnel wall corrections". *AGARDograph 109*, 1966.

[2]Karou, A. "Separated vortex flow over slender wings between side walls - theoretical and experimental investigation". *Report LR-300, Dept. of Aerospace Engineering, Delft University of Technology*, 1980.

[3]Engineering Sciences Data Unit. "Blockage corrections for bluff bodies in confined flows". *Item 80024, London*, 1980.

[4]Weinberg, Z. "Effect of tunnel walls on vortex breakdown location over delta wings". *AIAA Journal*, 30(6), June 1992.

[5]Thompson, S. A., and Nelson, R. C. "Wind tunnel blockage effects on slender wings undergoing large amplitude motions". *AIAA-92-3926*, July 1992.

[6]Pelletier, A., and Nelson, R. C. "Factors influencing vortex breakdown over 70^o delta wings". *AIAA-95-3469-CP*, 1995.

[7]Verhaagen, N. G., Houtman, E. M., and Verhelst, J. M. "A study of wall effect on the flow over a delta wing". *AIAA-96-2389*, 1996.

[8]Allan, M. R., Badcock, K. J., and Richards, B. E. "A CFD Investigation of wind tunnel wall influences on pitching delta wings". *AIAA-2002-2938*, June 2002.

[9]Hummel, D. "Untersuchungen über das Aufplatzen der Wirbel an schlanken Delta Flügeln". *Zeitschrift für Flugwissenschaften*, 13(5):158–168, 1965.

[10]Taylor, G., Gursul, I., and Greenwell, D. "Static hysteresis of vortex breakdown due to support interference". *AIAA 2001-2452*, 2001.

[11]Straka, W. A. "Effect of fuselage on delta wing vortex breakdown". *J. Aircraft*, 31(4):1002–1005, 1994.

[12]Ericsson, L.E. "Effect of fuselage geometry on delta-wing vortex breakdown". *J. Aircraft*, 35(6), November-December 1998.

[13]Ericsson, L. E. "Further analysis of fuselage effects on delta wing aerodynamics". *AIAA 2000-0891*, January 2000.

[14]Badcock, K. J., Woodgate, M., Stevenson, K., Richards, B. E., Allan, M., Goura, G. S. L., and Menzies, R. Aerodynamics studies on a Beowulf cluster. In P. Wilders et al., editor, *Parallel Computational Fluid Dynamics Practices and Theory*, pages 39–46, May 2002.

[15]Gordnier, R. E. "Computational study of a turbulent delta-wing flowfield using two-equation turbulence models". *AIAA 96-2076*, 1996.

[16]Brandsma, F. J., Kok, J. C., Dol, H. S., and Elsenaar, A. "Leading edge vortex flow computations and comparison with DNW-HST wind tunnel data". *RTO / AVT Vortex Flow Symposium, Loen, Norway*, 2001.

[17]Wilcox, D. C. "Turbulence modelling for CFD". *DCW Industries, Inc., La Cañada, California*, 1993.

[18]Allan, M. "A CFD Investigation of wind tunnel interference on delta wing aerodynamics". *Ph.D. Thesis, University of Glasgow, Glasgow, UK*, October 2002.

[19]Mitchell, A. M. "Caractérisation et contrôle de l'éclatement tourbillonnaire sure une aile delta aux hautes incidences". *Thèse de doctorat de l'Université Paris 6*, 2000.

[20]Visbal, M. R., and Gordnier, R. E. "Compressibility effects on vortex breakdown onset above a 75-degree sweep delta wing". *J. Aircraft*, 32(5):936–942, September-October 1995.

[21]Visbal, M. R. "Onset of vortex breakdown above a pitching delta wing". *AIAA Journal*, 32(8):1568–1575, August 1994.

[22]Sarpkaya, T. "On stationary and travelling vortex breakdowns". *J. Fluid Mech.*, 45(3):545–559, 1971.

[23]Visser, K. D. and Nelson, R. C. "Measurements of circulation and vorticity in the leading-edge vortex of a delta wing". *AIAA Journal*, 31(1):104–111, January 1993.

[24]Johari, H. and Moreira, J. "Direct measurement of delta-wing vortex circulation". *AIAA Journal*, 36(12):2195–2203, December 1998.

[25]Taylor, G., Gursul, I., and Greenwell, D. I. "An investigation of support interference in high angle of attack testing". *To appear in AIAA conference proceedings, RENO NV, USA*, January 2003.

[26]Sarpkaya, T. "Effect of adverse pressure gradient on vortex breakdown". *AIAA Journal*, 12(5):602–607, May 1974.